The Amt/MEP/Rh Family: Structure of AmtB and the Mechanism of Ammonia Gas Conduction

Shahram Khademi and Robert M. Stroud

Physiology 21:419-429, 2006. doi:10.1152/physiol.00051.2005

Physiology (formerly published as News in Physiological Science) publishes brief review articles on major physiological developments. It is published bimonthly in February, April, June, August, October, and December by the American Physiological Society, 9650 Rockville Pike, Bethesda MD 20814-3991. ISSN: 1548-9213, ESSN: 1548-9221. Visit our website at http://www.the-aps.org/.

PHYSIOLOGY 21: 419–429, 2006; 10.1152/physiol.00051.2005

The Amt/MEP/Rh Family: Structure of AmtB and the Mechanism of Ammonia Gas Conduction

Shahram Khademi
and Robert M. Stroud
Department of Biochemistry and Biophysics,
University of California-San Francisco,
San Francisco, California
stroud@msg.ucsf.edu

The atomic structures of the first members of the Amt/MEP/Rh family show that they are 11-crossing membrane proteins that form trimers in the membrane. Each monomer supports a hydrophobic channel that conducts NH_3 but not any water or ions. The reprotonation of NH_3 on the receiving side raises the pH on that side in the absence of metabolism of NH_3, and there is no transfer of protons through the protein.

Transport of ammonia across biological membranes is a key physiological process throughout all domains of life (7, 31, 32, 46, 60, 68), and most species have multiple different proteins of the family, underlining the importance of their roles in biology. Although NH_3/NH_4^+ (termed Am) is highly toxic to animals, it is the preferred source of nitrogen for most microorganisms. Once inside the cell, Am is directed to glutamine synthetase, which rapidly uses NH_3 as substrate to synthesize the amino acid glutamine using ATP. Thus metabolism serves to maintain an inward gradient of the substrate. In this article, we review the current state of knowledge of the mechanism of conductance, beginning with the structure of Amts, the mechanistic implications of these structures, experimental tests of the mechanism, and implications for the other family members, including the Rh proteins of clinical importance.

Nomenclature and Diversity of NH_3 Channels

Am exists in two forms, NH_4^+ and NH_3, in an equilibrium controlled by a pKa of 9.25 in aqueous solution. However, a hydrophobic environment can reduce the pKa to favor the neutral form in the equilibrium. Neutral NH_3 can diffuse through hydrophobic membranes and indeed can support growth of microorganisms, although when only low concentrations of Am are available, other regulated mechanisms of Am transport are used. *Escherichia coli* incorporates a single Amt (ammonium transporter) called AmtB carried on the *glnK amtB* operon. AmtB is barely expressed unless ammonium becomes growth limiting, whereupon the gene is induced. In bacteria, ammonia transporters in the family are termed Amts. Three are found in yeast and called methylammonium/ammonium permeases or MEPs. Ammonia is an important source of nitrogen for plants (21), and in plants they are termed Amts (51). Three Amts are found in tomato (33), three are found in *Arabidopsis* (15), others are found in rice (71). Amts are also found in invertebrates. The *Caenorhabditis elegans* genome, for example, contains four Amt homologs.

Members of the Rh branch of the family are found in animals, sometimes alongside Amts in invertebrates, but not so in mammals. The human erythrocyte carries the Rh proteins RhD and RhCcEe that express the antigens of the red blood cell and RhAG in complex, whereas RhBG and RhCG are found in kidney, brain, and many organs. In mammals, Am transport is vital to kidney physiology in maintaining pH and in renal ammonia secretion (30).

Marini and colleagues show, based on the partial functional complementation by Rh proteins of an *S. cerevisiae* Δ(*mep1,2,3*) mutant in which all three MEPs are deleted, that the Rh50, Rh-associated glycoproteins RhAG, RhBG, and RhCG can likewise conduct Am (43, 44). Since the structure determination of AmtB and alignment of the sequences of RhAG, RhBG, and RhCG especially show conservation of critical components with AmtB, which suggests they are structurally and functionally similar to AmtB (8, 29). Interestingly, invertebrates, and notably the green algae *Chlamydomonas*, have both Amts (of which there are four) and members of the Rhesus protein branch (Rh proteins, of which there are two) (32). Physiological considerations led Soupene et al. to propose that the function of Rh proteins might include transport of CO_2 as diffusive channel (62). It has since been shown that RhAG and AmtB can indeed conduct both NH_3 and CO_2 (48).

Structure of Amts: The Paradigm for the Family

The X-ray structure of AmtB from *E. coli* was initially determined to 1.3 Å resolution at pH 6.8, with and without Am or MA (29). The structure shows that the protein is an 11-crossing membrane protein that homotrimerizes in a threefold symmetric fashion. Each monomer incorporates a hydrophobic channel in between relatively polar cytoplasmic and periplasmic vestibules. This, and "difference mapping" between pairs of the structures in presence of MA or Am, and the crystals of AmtB without any Am suggested that it recruits ammonium ions, the most available Am species

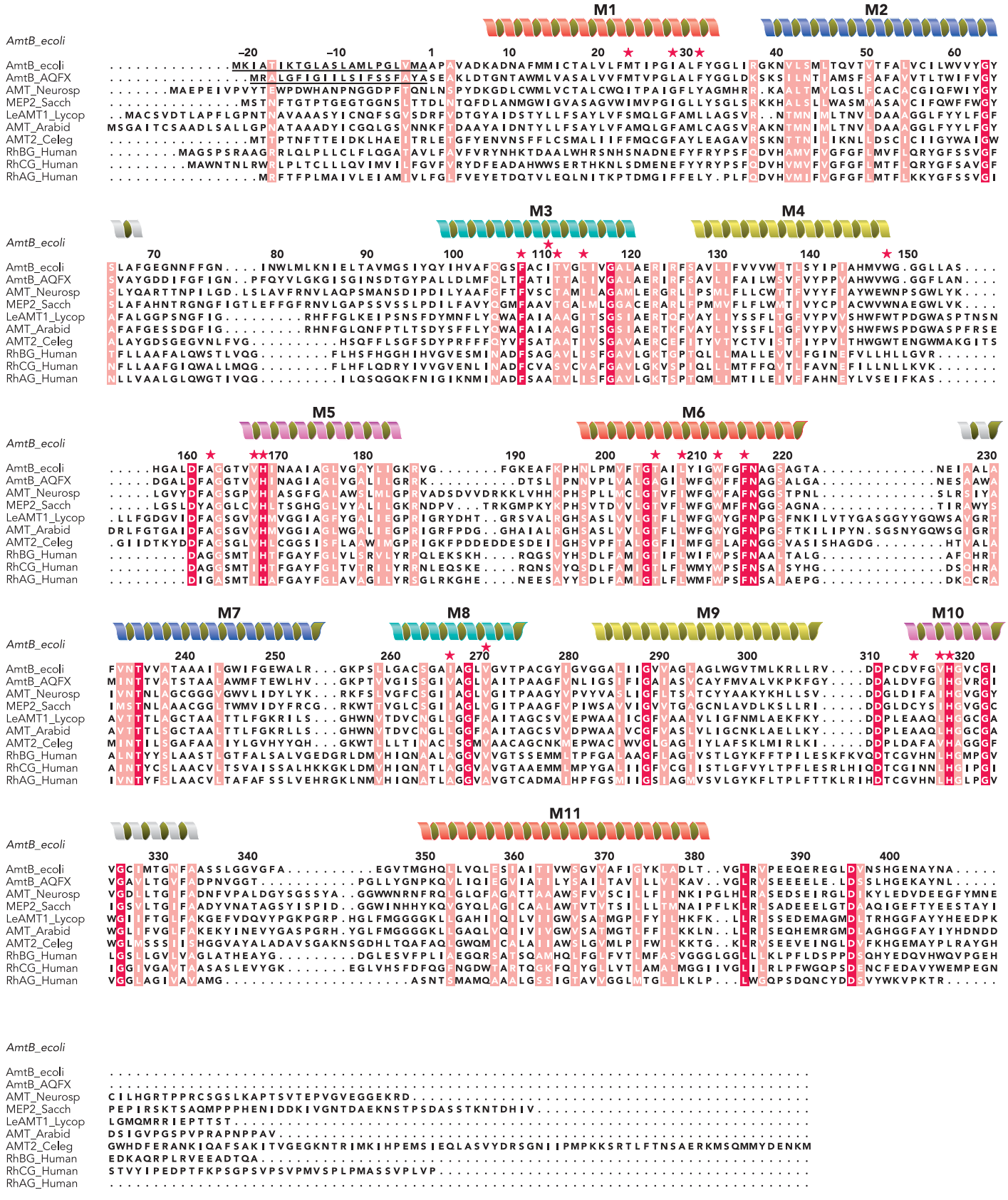

FIGURE 1. **Sequences of AmtB/MEP/Rh homologs from *E. coli*, *A. aeolicus*, *Neurospora Saccharomyces cerevisiae*, *Lycopersicon esculentum*, *Arabidopsis thaliana*, *Caenorhabditis elegans*, and human Rh proteins**
Trans-membrane helices M1–M11 are indicated. The numbering is that of *E. coli* AmtB. Conserved amino acids are in white in red-filled rectangles. Similar residues are in red surrounded by blue lines. The signal sequences in *E. coli* and *A. aeolicus* are underlined. Red stars indicate residues that line the lumen of the channel.

at pH of <9, but conducts only neutral NH_3, leaving a proton behind, a mechanism supported by assays of AmtB reconstituted in proteoliposomes (29). The structure was independently determined to 1.8 Å at pH 4.6 and compared with our first-reported structure (76). A third structure of Amt-1, one of three Amts from the hyperthermophilic archaeon *Archaeoglobus fulgidus*, was later determined at 1.54 Å (3).

NH_2-terminal amino acid sequencing of AmtB shows that 20 amino acids are excised from the NH_2-terminus of *Aquifex aeolicus* AmtB (AmtB_AQFX), whereas 22 residues are cleaved from the *Escherichia coli* AmtB (AmtB_Ecoli) in the mature proteins (29). These are signal sequences that were appropriately cleaved during expression in *E. coli*. They are strongly predicted to be signal sequences using neural network approaches (50) (FIGURE 1). Thus the AmtB monomer (FIGURE 2A) is comprised of 11 transmembrane helices with the NH_2-terminus on the periplasmic side and the COOH-terminus on the cytoplasmic side (29). The trimer (FIGURE 2B) is also quite stable, even running as a trimer in SDS-PAGE, and the trimer is the physiological form of the protein (6, 9).

Consistent with the "positive inside" trend in membrane proteins, the trimer of AmtB_Ecoli has net negative charge of –7.5 (13.5 positive + 21 negative) on the periplasmic surface and net positive charge of +9 (42 positive + 33 negative) on the cytoplasmic side. Several side chains of tyrosine and tryptophan with their partially polar character lie in positions to interact with the lipid head groups around the trimer.

To date, the 11-crossing structure of AmtB (and we presume of the associated MEP/Rh proteins) is the first of this fold among membrane proteins. It reveals a quasi-twofold symmetric structure within the monomer itself, in which membrane-spanning segments M1–M5 are related to M6–M10 by a quasi-twofold axis that lies in the mid-membrane plane. The implied gene duplication presumably occurred before the transport function arose since the two related domains are oppositely polarized with respect to the sidedness of the membrane. Alternatively, the primordial gene product before the duplication may have been of the type that could adopt either polarity in the membrane to form a functional anti-parallel dimer. This kind of alternate topology has recently been proposed to occur in membrane proteins based on fusion protein labels for determination of factors that control sidedness of membrane proteins (56). The final helix M11 is long and highly inclined to the membrane and lies on the outer surface of the trimer, in contact with the lipids. Together M1–M10 diverge outward from the central plane in a right-handed helical bundle to generate a vestibule on each side of the cell membrane (FIGURE 2, A AND B).

Such structural duplications with opposite polarity are increasingly seen in other membrane protein structures, including GlpF and the aquaporins (14, 18, 61, 66), the SecY protein of the translocon (69), the ClC H^+-Cl^- exchange transporter (2, 11, 12), the bacterial homolog of the Na^+/Cl^--dependent neurotransmitter transporters for biogenic amines (75),

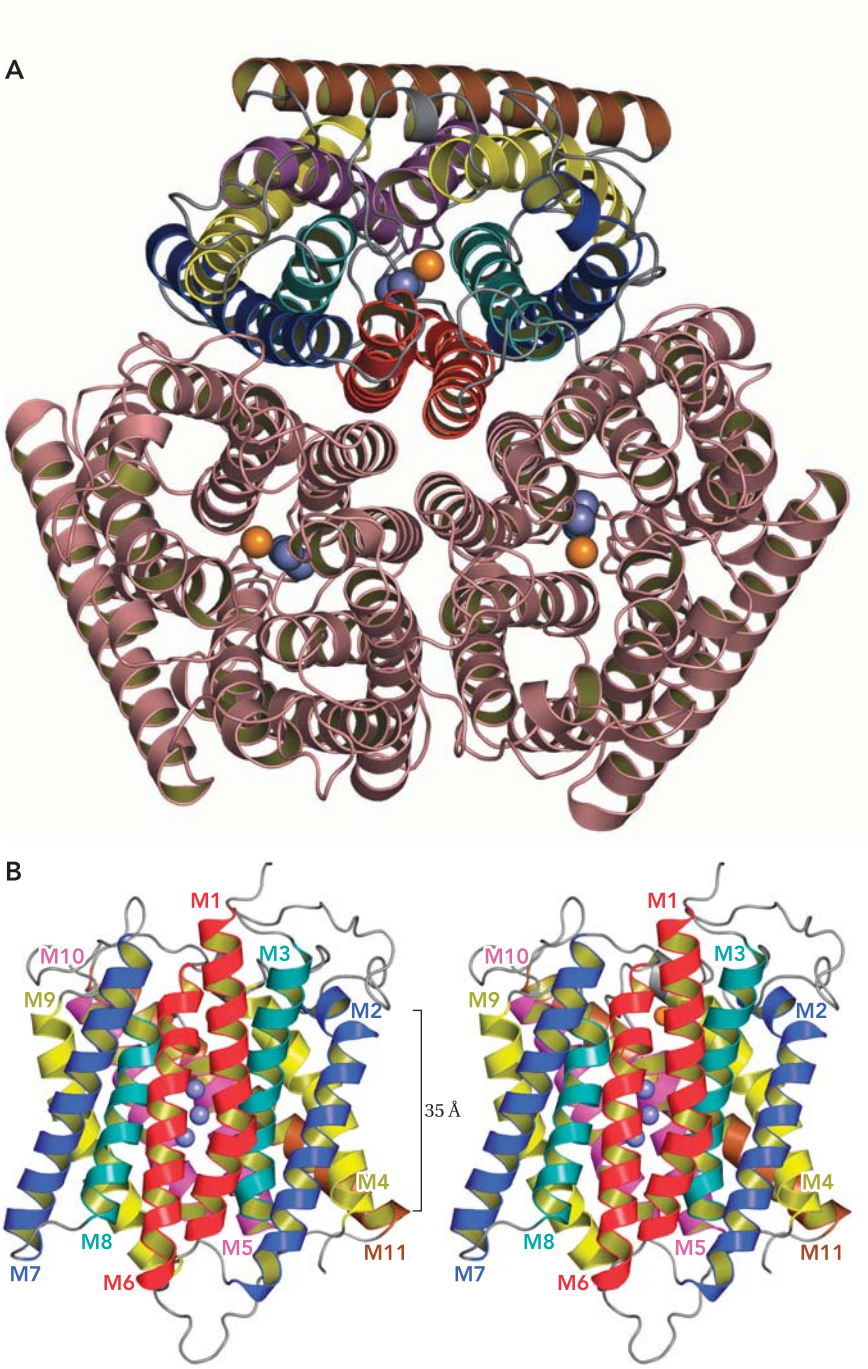

FIGURE 2. **The three-dimensional fold of AmtB**
A: stereoscopic view of the monomer ammonia channel viewed down the quasi-twofold axis with the extracellular side uppermost. The vertical bar (35 Å) represents the inferred position of the hydrophobic portion of the bilayer. Three NH_3 molecules, seen only when crystallized in presence of ammonium sulfate, are shown as blue spheres. *B*: ribbon representation of the AmtB trimer is viewed from the extracellular side. A threefold axis perpendicular to the page relates the three monomers. In the top monomer, the quasi-twofold axis is vertical and parallel to the plane of the page and relates the five-helix motif on the left side to the five-helix motif on the right. Corresponding quasi-twofold-related helices are shown in the same color. The quasi-twofold axis intersects the threefold axis; thus each motif fulfills a similar role in building the interfaces between monomers. The blue spheres are potential ammonia molecules. The orange sphere represents an ammonium ion.

and lactose permease LacY (1), GlpT (22), and their "major facilitator super-family" (MFS) homologs. The vestiges of structural duplication were recognized in the gene sequences of the aquaporins (53) and in the MFS (52) before structure determination, although not in the Amt/MEP/Rh superfamily. In hindsight, one could imagine algorithms that could detect such gene duplication based on the increasingly good ability to predict the topography of membrane-spanning segments (16) and the expectation that the duplicated segments would retain some structural similarity.

In light of the structure of AmtB, the highly conserved residues Asp 160 (7 residues) His168 at the NH_2-terminal end of M5 and Asp 310 (7 residues) His 318 located 150 residues downstream at the NH_2-terminal end of M10 are some of the most notable vestiges of duplication in the amino acid sequences.

The Mechanism of NH_3 Conduction Deduced from the Structure

To probe the mechanism of conductance, 25 mM $AmSO_4$ at pH 6.5 or 100 mM $MASO_4$ at pH 6.5 was added to crystals of AmtB to see whether there were any discreet binding sites for Am/MA (29). No significant conformational changes are induced, suggesting that AmtB acts as a channel that serves to conduct Am in the direction of an Am gradient. Subsequently, we developed biochemical assays with AmtB reconstituted into liposomes (proteoliposomes) to test and validate our deduced mechanism.

The conducting pathway within each monomer of AmtB lies between two vestibules, one on the outer surface and the other on the cytoplasmic surface (FIGURE 3A). Each vestibule contains approximately 30 sites occupied by water molecules that are hydrogen bonded to one another and to the carbonyls and

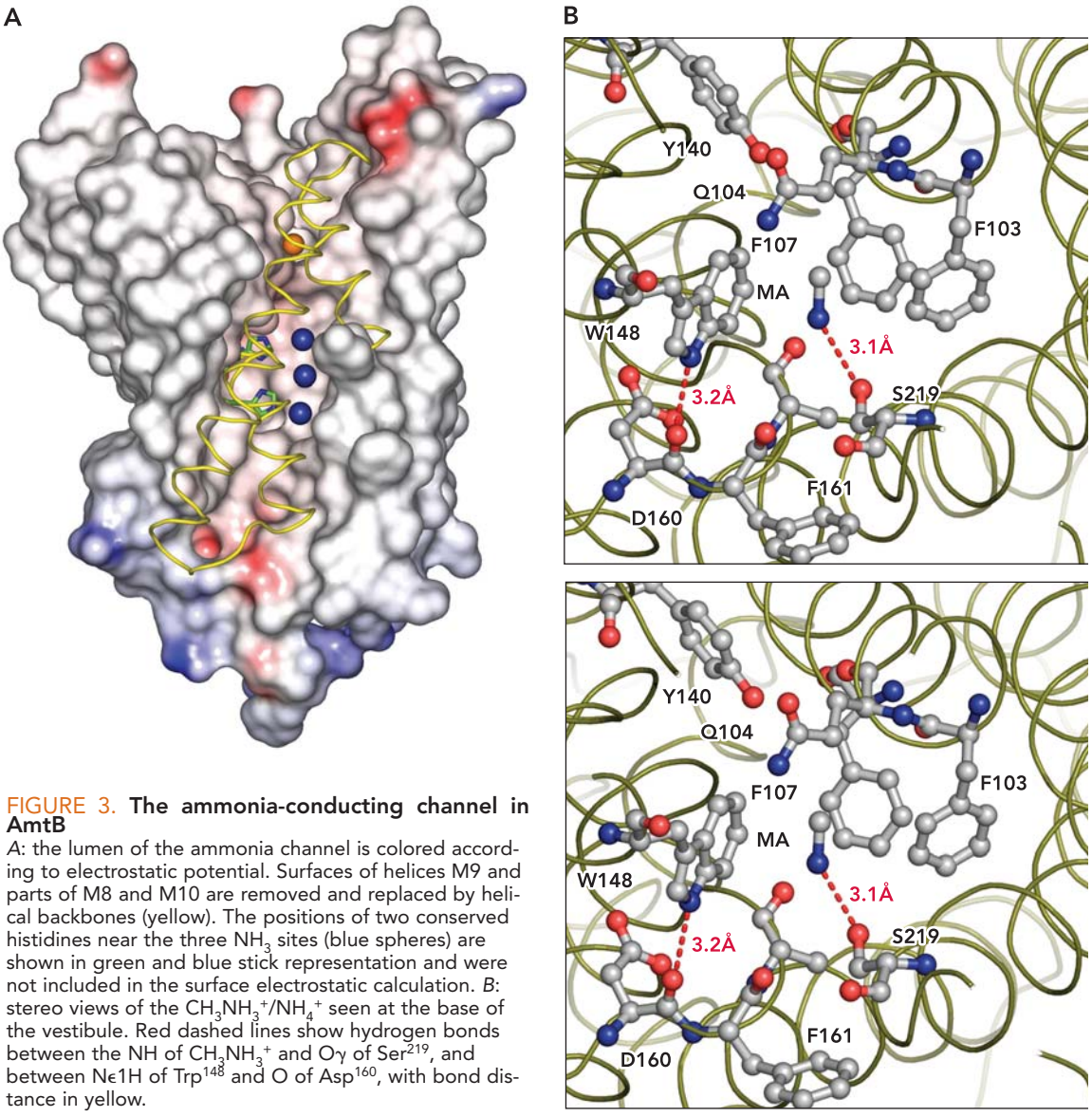

FIGURE 3. **The ammonia-conducting channel in AmtB**

A: the lumen of the ammonia channel is colored according to electrostatic potential. Surfaces of helices M9 and parts of M8 and M10 are removed and replaced by helical backbones (yellow). The positions of two conserved histidines near the three NH_3 sites (blue spheres) are shown in green and blue stick representation and were not included in the surface electrostatic calculation. *B*: stereo views of the $CH_3NH_3^+/NH_4^+$ seen at the base of the vestibule. Red dashed lines show hydrogen bonds between the NH of $CH_3NH_3^+$ and Oγ of Ser^{219}, and between Nε1H of Trp^{148} and O of Asp^{160}, with bond distance in yellow.

polar groups in the vestibules. Between the vestibules, the lumen is narrow and mostly formed by aliphatic nonpolar side chains throughout its approximately 20-Å length. This would only seem consistent with conduction of a neutral molecule such as uncharged NH_3. To test the hydrophobic nature of the pore, a hydrophobic gas, xenon, was diffused into the crystals of Amt-1. Two xenon atoms were found in the lumen of the pore, emphasizing the hydrophobicity of the substrate channel (3).

There is no discreet water visible in the lumen, even though the structure is at 1.35-Å resolution, which is almost sufficient to resolve the positions of hydrogen atoms (29). This could be because any water is in dynamic motion or it could be because the lumen is too hydrophobic to retain or transport water. We surmise that it is probably the latter, since no water is conducted by the channel (29). The single exception to the hydrophobic walls lies on either side of the mid-membrane center of the pathway where there are two inline, almost coplanar imidazole side chains of H168 and H318. The two are hydrogen bonded to one another, and they are highly conserved throughout the AmtB/MEP/Rh family (although not in erythroid RhCcEe and RhD).

The entrance to the lumen has a narrow 1.2-Å diameter hydrophobic constriction on each side that must move apart dynamically during any conduction event. This necessity for a dynamic opening to allow entry to and exit from the hydrophobic portion of the pathway does not change the inference that the protein acts as a diffusive channel. Likewise, the relatively low flux for ammonia for a channel, estimated from various free-energy calculations to be $<10^4$/s (76), may reflect these dynamic structural and electrostatic barriers to NH_3.

Since X-rays are scattered by electrons, it is difficult to "visualize" NH_3 vs. NH_4^+, H_2O, Na^+, Mg^{2+}, or even F^- since all of these species have the same electron content of 10 electrons. Thus any possible binding site for Am could only be defined using the alternate substrate, methyl ammonium. In the presence of MA, there is one partially occupied MA site seen in a "difference electron density map" (29). However, even though the MA concentration (100 mM) is 2,000-fold higher than levels that would reach 50% maximal conduction rate [K_m (MA) ~50 μM], the site is only 60% ordered, reflecting the fact that it is not rigidly held in place but rather is an electrostatically favorable location for the Am-related cations. That is to say that there is no real binding site as such, although this site, located at the very bottom of the vestibule as it enters the hydrophobic portal to the lumen, may be on the pathway and help catalyze the removal of a proton from ammonium ion, to yield the neutral NH_3 for transport.

Interestingly, this "recruitment" site is located against three aromatic rings of F103, F107, and W148 and allows a hydrogen bond to Ser219. The π-electron orbitals within such aromatic rings provide for a so-called "π-cation site," favorable for cations such as NH_4^+ and CH_3 NH_3^+ (FIGURE 3B). The K_m (Am) for transport of Am is approximately 10 μM, and, in presence of 25 mM Am rather than MA, a 67% occupied peak lies in the π-cation site. There is a similar well-defined H_2O peak at this site in the absence of Am. Overall, the site may help catalyze the deprotonation of the ammonium ion as it proceeds on to the hydrophobic lumen that then acts as a channel for NH_3. Each vestibule offers approximately eight carbonyl oxygens (each with δ–0.4e charge) to act as an attractive funnel for water and for positively charged NH_4^+. The idea that this "recruitment" site may act as a transient site in the mechanism is consistent with the finding that there is competition between Am and MA (26) for transport, which can also be competed by nontransported dimethylamine or ethylamine (45). Interestingly, K^+ or alkali cations do not compete with NH_3 transport.

In $AmSO_4$ vs. no Am present, three weakly occupied sites (Am2, Am3, and Am4) lie adjacent to imidazole rings of conserved quasi twofold related His168 and His318 and hint at transient intermediate sites along the pathway (FIGURE 4). On average, these peaks indicate only approximately 20% occupancy at each site (approximately 1.4 electrons each), so they provide a lower limit to the occupancy by NH_3. There are suggestions that these weak peaks may be water and seem to be observed at pH 4.6 with or without NH_3 (3, 76). However, the peaks have such low occupancy and are most sensitively quantitated in the difference between protein with Am and protein without Am. In addition, we show that water is not conducted by AmtB (29); thus it is unlikely that there is any even disordered water in the channel. There are at best only very weak hydrogen bonds to Am2, Am3, and Am4 from the Cε1-H of the imidazole rings of His168 to Am2 (3.2 Å) and from His318 to Am3 (3.4 Å). We presume that these histidine side chains are neutral since they lie in the hydrophobic lumen with no evidence of ordered water for solvation nearby. Since they are hydrogen bonded together between Nδ of H168 and Nδ of H318, sharing one hydrogen atom, they could not both be protonated without moving apart quite significantly. It is most likely that their conjoint pKa is significantly lowered by the environment to preserve their neutrality within the hydrophobic lumen. Indeed, the structure at pH 4.6 shows no difference in this low dielectric environment, suggesting that the pKa may be below pH 4.

In general, for example, in enzyme active sites, imidazoles of histidine often facilitate acid-base mechanisms with their pKa when solvated near 6.8. The conservation of these residues leads one to query the possibility of a role in proton removal from NH_4^+ by the two-imidazole pair. The pair of imidazoles might somehow facilitate removal or conceivably rotate to pass such a proton on through the lumen and eventually reprotonate the NH_3 at the end of its travel. This

cannot yet be absolutely excluded as an occasional event; however, the predominant species going through the channel is NH_3, without any accompanying water molecules, as we discuss below.

Asp 160 and Asp 310 are both highly conserved and occur just seven residues ahead of the two conserved histidines. Mutation of conserved Asp160 to Ala160 abrogates transport of MA, implying that it plays a key role (25). Asp160 and 310 are not accessible to bulk solvent in the structure, and their role appears to be a key structural role. Conserved Asp160 is a helix-capping residue for M5, whereas Asp310, the conserved quasi twofold relative of Asp160, similarly acts as a helix cap for M10. However, molecular dynamics simulations suggest that there may be a structure change that allows Asp160 (and, by our inference, Asp 310) to become solvent accessible in the vestibule and act as the ultimate base assisting in proton removal from NH_4^+ (36).

Biochemical Assay of Purified Reconstituted Protein

To test the substrate specificity and rates of conductance of AmtB, a fluorescence-based assay was adapted to measure influx of ammonium into proteoliposomes using pH-sensitive 5-carboxyfluorescein (CF) inside the vesicles (29, 54, 59). Rapid mixing of carboxyfluorescein-loaded vesicles in buffer with ammonium chloride (0.5 mM or 5 mM) was initiated at pH 6.8 in a stopped-flow spectrometer. NH_4^+ is in equilibrium with NH_3 with a pK_a of 9.25 in aqueous solution. Any influx of NH_3 would reacquire a proton inside forming NH_4^+ and OH^- and so raise intravesicular pH. The addition of 5 mM NH_4Cl outside led to a rise in pH with a rate of 115.6 ±13.2 s^{-1} ($n = 6$) that was >10-fold higher when AmtB was incorporated vs. 12.8 ±0.7 s^{-1} ($n = 6$) for protein-free liposomes. This clearly implies that, indeed, NH_3 is transported to equilibrium, down the concentration gradient. It gains a proton inside the proteoliposomes to raise the pH inside the proteoliposomes.

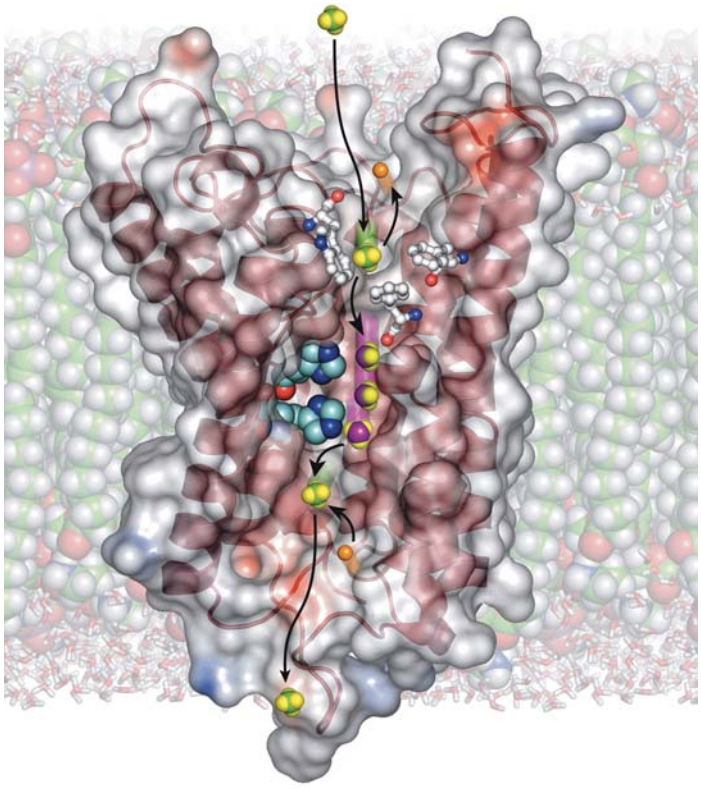

FIGURE 4. **The mechanism of conductance of NH_3**
The green and purple spheres are nitrogen atoms of NH_4^+ and NH_3, respectively. The mechanism involves an extracellular vestibule attracting Am, a vestibule that can attract NH_4^+, and a hydrophobic channel that strips the proton (orange spheres) off the NH_4^+ to conduct just NH_3. NH_3 is reprotonated on the cytoplasmic site to reform NH_4^+ and H_2O.

To further clarify, in this carefully controlled experiment, the vesicles are first loaded with the carboxyfluorescein, then washed and spun down twice. The rise in fluorescence with the increase in pH is small, and thus that change is normalized to 1.0 to plot the change in "relative fluorescence" (29) vs. time, and the entire reaction is complete within fractions of a second. The pH of the vast volume on the outside of the vesicles does not change. Thus any fluorescence change reflects only what takes place inside the liposomes. Any dye that might have remained on the outside of the vesicles does not change on addition of $AmSO_4$. The diffusion of NH_3 is much faster than for the bulky carboxyfluorescene molecule and is complete within 0.1–0.4 s. Likewise, any leakage of dye out of the proteoliposomes would change only the magnitude of the small change, the "signal" but not its time dependence. The lack of any drift in this value over the relevant time scale shows that leakage is in any case not a factor. This was verified by replacing $AmSO_4$ by NaCl as a control. Using NaCl did not cause any change in relative fluorescence (29), and this also shows that the fluorescence change is not because of leakage of dye out of liposome.

To see whether water passed through AmtB, we again used the fluorescence of carboxyfluorescein. This time, the concentration of dye was monitored by its alteration in self-quenching vs. time. Indeed, the AmtB proteoliposomes show no difference from liposomes in their rate of water conductance, as reflected in response to an osmotic challenge using sucrose, showing that essentially no water passes through the hydrophobic channel (29).

The Mechanism Deduced from Structure

The mechanism therefore involves the following elements: a site that can recruit and possibly assist in deprotonation of NH_4^+ and a hydrophobic channel for NH_3 that must lower the pKa of Am, probably to a very low level ensuring that it is always in its gas-like neutral form inside the hydrophobic portion. The energy to accomplish lowering of pKa, perhaps by as much as 8 pH units, perhaps approximately 12 kcal/M is

already much less than the cost of dehydrating an NH_4^+ ion. Thus the hydrophobic channel, and its affinity for hydrophobic NH_3, coupled with the lack of any water of hydration within, easily suffices. Put another way, the dehydration of NH_3 is much more easily accomplished than the dehydration of the NH_4^+ ion. This difference in energy easily reaches that required to accommodate the necessary change in pKa. From our observations that were made at pH 6.8, solely to exploit the most sensitive region of the fluorescent dye, the pKa of the NH_3 when it is in the channel must be pKa < 6. It is probably much lower. Once it leaves the channel, the pKa reverts to its aqueous value and takes up a proton to yield $NH_4^+ + OH^-$, thus raising the pH inside the proteoliposomes.

All the observations noted so far are reconciled by the recruitment of NH_4^+, reduction of its pKa, and conductance of NH_3 as the primary mechanism. In some ways, the proton-stripping mechanism we propose makes it seem as if a proton is transferred from inside to outside since NH_4^+ leaves a proton starting on the outside, to pick one up on the other side. Unlike an antiporter, however, there would be no net transfer of a proton.

One problem that has been raised with this mechanism is that it would tend to alkalinize the cell, effectively removing protons from inside to outside against the normally 0.2-V proton motive force across the plasma membrane in *E. coli*. If so, the process would cease to work. This would only work either if the NH_3 were metabolized as NH_3 rather than NH_4^+, which it is by GS, or if there was an energy source that helped to drive the process. GS is the enzyme that provides the source of energy by ATP hydrolysis that serves to fix the NH_3 into glutamine and maintain the inward gradient of NH_3.

Chemistry of NH_3 Transport

Based on the growth behavior of both enteric bacteria and *S. cerevisiae*, the Kustu group proposed that AmtB/MEP proteins and their homologs increase the rate of diffusion of the uncharged species NH_3 across the cytoplasmic membrane and deduced that there was no evidence for concentrative uptake of NH_3 against a gradient (63, 65). This is now borne out by the flux assay of purified AmtB in reconstituted liposomes (29). This shows that the channel is indeed a passive channel that conducts NH_3 bidirectionally in the absence of any energy source. Seeking a direct measure of conduction rates in vivo, and since the radioactive nitrogen isotope is very short lived, transport rates of most Amt/MEP proteins has been monitored by transport of radioactive ^{14}C-labeled $CH_3NH_2/CH_3NH_3^+$ (termed MA) (17). When carried out in vivo, this [^{14}C]MA assay has led to misunderstandings in the past, since at least in *E.coli* [^{14}C]MA is converted into [^{14}C]methylglutamine by glutamine synthetase (26, 63); thus, before this realization, accumulation of radioactivity erroneously appeared to be a concentrative MA uptake against a gradient, which sometimes led incorrectly to suggestions of active, energy-coupled, or electrogenic transport through the transporter. Consequently, experiments that rely on conductance of [^{14}C]MA need to be reevaluated.

A modification of the method (27) was generated by the Merrick group to yield the activity of AmtB alone and shows AmtB to act as a slow diffusive channel (26). It was also shown that transport is not dependent either on membrane potential or on ATP, which thereby supercedes other attempts to monitor [^{14}C]MA uptake using protonophores like CCCP or adjustments of membrane potential.

The dependence of MA uptake by AmtB on external pH was shown to increase by a factor of 2.7, between pH 6.25 and pH 7.25, and by a factor of 3.8, between pH 7.25 and pH 8.25 (26). This factor of approximately 10 between pH 6.25 and 8.25 does not correspond to the approximately 100-fold change in concentration of NH_3 in the bulk solution, as had been implied by Soupene (63). It therefore invalidates the notion that NH_3 from the bulk solution is conducted and supports the mechanism deduced from the X-ray crystal structure of AmtB in which NH_4^+ is recruited into the periplasmic vestibule and deprotonated to allow NH_3 to pass through the channel (29).

Insightfully, the Merrick group took advantage of this observation to show that the apparent K_m of the substrate MA for GS is much lower in vivo (K_m = 380 μM) than it is for the enzyme in isolation (K_m = 79 mM). They infer that AmtB and multiple allosterically regulated GS may be metabolically coupled together in some way (24). This makes sense since the GS reaction uses NH_3 as substrate and thus bypasses any tendency of the NH_3 transport to change the pH inside the cell. Physical proximity would help channel the substrate more directly to the enzyme and maintain the inward gradient of NH_3. Arrhenius plots for GS indicate activation energy of 14.1 kcal/M. The energy of activation (E_a) for AmtB was 1.6 kcal/M, consistent with its action as a slow channel for NH_3.

Simulation of Conductance by AmtB

Molecular dynamic simulations of Am transport through AmtB support the role of the recruitment site in the vestibule (36), which is followed by passage of neutral NH_3 through the hydrophobic pathway. Specifically, these calculations show a quite small E_a of 3.1 kcal/M for NH_4^+ ion as it enters the vestibule, which compares well with the measured 1.6 kcal/M at 37°C (26). "Molecular mechanics" are an important guide as to whether processes deduced from static or "time-averaged" crystal structures can take place, and in what time scale. They bridge the time-averaged crystal structure and biochemical assays to test mechanism

by means of simulation in a computational environment. The simulations of AmtB show how a hydrogen bond to NH_4^+, first with the backbone carbonyl oxygen of Phe161 then with the hydroxyl group of Ser219, compensate for the loss of a hydrogen bond to water and how the aromatic rings of Trp148 and Phe107 assist in the π-cation interactions. At the end of the vestibule, the phenyl ring of Phe107 dynamically switches to an open state accompanied by a slight rotation and shifting of the indole ring of Trp148. This allows access of the initially buried and highly conserved carboxylate group of Asp160 to the vestibule, where it may become the base that ultimately helps catalyze the deprotonation of NH_4^+ via water molecules (36). This might be a second reason for the high conservation of Asp160 and its twofold counterpart Asp 310 in Amt proteins and could be a factor in why the D160A mutant (25) or D160N in MEPs, RhAG, and RhCG are inactive as transporters (42). Once NH_4^+ deprotonates, the phenyl ring of Phe215 rotates to open, and the subsequent passage of NH_3 through the channel is straightforward.

Regulation of Ammonia Transport

In most bacteria, Amt genes are induced by nitrogen limitation, which is controlled by an activator, NtrC. However, PII signal transduction proteins that can also block transport also tightly regulate nitrogen metabolism posttranslationally. In almost all bacteria, the *amtB* gene is linked to *glnK* (67). GlnK inhibits NH_3 transport by direct association with AmtB. Inhibition by GlnK is controlled by the uridylylation/deuridylylation of GlnK. GlnK is also a trimeric but soluble protein that binds to the AmtB trimer and blocks conduction directly (10, 46). Each of three PII-like encoding genes, paralogs *glnB*, *glnK* (*GlnK1* and *GlnK2*), and *glnY* are found in close association with Amts. In each case, the unmodified protein is inhibitory. Models of this assembly have been made (3) and, along with structure determinations, show how association prevents NH_3 progressing through the cytoplasmic side of the channel. The COOH terminal 20 amino acids of *E. coli* AmtB are extremely polar, highly charged, and, not surprisingly, not ordered in the structure. They are likely to be involved in the regulatory interface with the PII-proteins (3).

Function and Structure of the Rh Proteins and Rh-Associated Glycoproteins

Rh found in animalia fall into a distinct branch of the Amt/MEP/Rh family. RhAG can specifically mediate ammonium transport when expressed in ammonium-uptake-deficient yeast by testing the growth of triple-*mepΔ* strains on media containing <5 mM ammonium (43). Expression of RhAG enhances resistance to a toxic concentration of methylammonium (250 mM) in such triple-*mepΔ* yeast, consistent with RhAG promoting export of the ammonia analog. Although bacteria, plants, and fungi can acquire nitrogen from their environment in the preferred form of ammonia (72), mammals prefer assimilated forms of nitrogen, amino acids, for nutrition, and they excrete nitrogen as Am mediated by Rh proteins (43).

Multiple Rh-associated glycoproteins are identified in various organs (73, 74). RhAG is expressed in erythrocytes and erythroid precursors along with the Rh proteins RhCcEe and RhD (5, 40), where it facilitates export of Am (19). Nonerythroid RhBG and RhCG are expressed in important sites for ammonia metabolism, including kidney, liver, skin, testis, the central nervous system, and the intestinal tract (4, 30, 39, 41, 49, 55, 73).

Based on the structure of AmtB and sequence conservation, the Rh-associated glycoproteins and the Rh proteins most probably have the same structural framework and trimeric state as AmtB, despite earlier suggestions that they had 12 crossings (13): the first helix M1 lies in the center of the trimer. Thus any portion of the protein that was coded for by sequences ahead of the mature NH_2 terminus of AmtB, or its homologous position in other proteins of the family, would be difficult to accommodate within the trimeric structure (FIGURE 2). Thus we propose that all of the Rh-associated glycoproteins, RhAG, RhBG, and RhCG, will also follow the same pattern with cleaved signal sequences and that they will form trimeric assemblies.

It is therefore worth reexamining the data again that suggested 12 crossings and a cytoplasmic NH_2 terminus. The conclusion was based on antibody binding of anti-peptide polyclonal Rh30A antibodies to intact red cells vs. to leaky red cells that opened access to the inside. The NH_2 terminus of a full-length protein was seen in Western blots to be on the cytoplasmic side. This remains a conundrum that is apparently confusing in the field. However, the signal sequence could have been only partially cleaved from Rh or it could have been cleaved from the functional protein and been left with the exposed epitope on the signal peptide, with its NH_2 terminus detectable only from the inside.

Like AmtB, the erythroid Rh proteins are usually oligomers of RhAG with Rh proteins RhCcEe and RhD (13, 57, 70). We would expect them to be trimers, but heterotrimers rather than the homotrimers of AmtB. By the principles of assembly, one would expect that a heterotrimer would contain three different proteins in a uniform arrangement. The erythroid Rh proteins that carry the antigenic sites RhCcEe and RhD are less similar to AmtB in that they do not conserve the second Asp 310 His 318 pair. The first pair is present but separated by only six amino acids vs. seven. Nevertheless, these proteins make a complex in the red cell with RhAG. The quaternary structure of this complex has been thought of as a tetramer; however, considerations of assembly would suggest that the

complex should be a unique arrangement of all three proteins in a heterotrimer.

A single Rh complex unit has been estimated to have a conductance of about 1–2 × 10^6 molecules NH_3/s consistent with action as a channel (58, 70). It has been suggested that Rh proteins, prominent in mammals that do not contain more Amt-like subfamily members, may function physiologically as the much sought-after channels responsible for CO_2 transport in the red cell (64). Recently, Boron and colleagues (48) showed that the red cell RhAG, and indeed AmtB, can conduct both NH_3 and CO_2. They also found that the red cell aquaporin AQP1, a water channel, also conducts CO_2 and NH_3. The ratios of CO_2 to NH_3 permeability indexes suggest that AQP1 is actually the most selective for CO_2 (2.8), whereas for AmtB the ratio is 0.98. For RhAG, it is 0.37.

Although AmtB and Rh have limited sequence conservation, the AmtB structure makes it possible to map the sequence of Rh onto the three-dimensional structure of AmtB in an attempt to further address questions of Rh function. Most particularly, the two motifs, residues D160, H168, and D310, H318, which are conserved in Amt/MEP proteins and play key roles with the histidines inside the hydrophobic channel of AmtB_Ecoli, are conserved in RhAG, RhBG, and RhCG. In RhD and RhCcEe, the first pair seems to be preserved (70). The aromatic residue at F107 is conserved; those at F103 and W148 are not and are aliphatic in RhAG, RhBG, and RhCG.

Water and Ammonia

AmtB has no measurable permeability for water. In contrast, some members of the water channels do conduct NH_3. AtTIP2;1 from *Arabidopsis* roots, an AQP homolog in plants, is unregulated in response to nitrogen starvation (38), suggesting that TIP2 functions in remobilization of ammonium from vacuoles by transporting ammonium across the membrane (23). Using functional complementation of a yeast mutant deficient in all three ammonium transporters (*Dmep1–3*) by wheat (*Triticum aestivum*) *TIP2* AQPs and also using expression in *Xenopus* oocytes, TaTIP2;1 and mammalian AQP3, AQP8, and AQP9 have been shown to conduct NH_3 (20, 23, 37). Such AQPs are called aquaammoniaporins. AQP3 is found in erythrocytes, and AQP8 and AQP9 are primarily found in nitrogen-handling organs such as the liver and the kidney.

Six high-resolution crystal structures of AQP homologs cover the various AQP subclasses (34), the aquaglyceroporin GlpF (14), AQP1 (66), AQPZ (61), AQP0 (18), and the probable H2S channel AQPM (35). In GlpF, the channel is slightly wider, and key hydrophobic residues allow the passage of the carbon backbone of glycerol. In pure water channels, the selectivity filter is surrounded by R197/F58/H182/C191. In the aquaammoniaporin TIPs, isoleucine or valine replace H182, and glycine or alanine substitute at C191. F58 of bovine AQP1 is substituted by histidine, tryptophan, leucine, and alanine in aquaammoniaporins. These substitutions make the selectivity filter in aquaammoniaporins wider and more hydrophobic. Both the dipole moment (1.49 for NH_3 vs. 1.85 for H_2O) and the dielectric constant of the liquid (22 for NH_3 vs. 80 for H_2O) are considerably lower than that of H_2O. A more hydrophobic selectivity region favors NH_3 transport in the AQPs. Likewise, mutation of the selectivity filter residues in TIP2;1 to the corresponding residues from AQP1 resulted in the loss of NH_3 conduction in TIP2;1 (23).

Since all K^+ channels also conduct the ionic form of NH_4^+ with similar ionic radius (0.148 vs. 0.149) and hydration shells, it is crucial that the mechanism of Amt/MEPs and Rh absolutely exclude K^+ ion leakage. Although the K^+ channels must conduct charged cations and mimic the hydration shell with oxygen (28, 47), ammonia channels utilize the titrateable character of ammonia to stabilize and then allow passage of the unhydrated NH_3, and thereby ensure that there is no leakage of any hydrated ions.

Research was supported by the National Institute of General Medical Sciences Grant GM-24485 to R. M. Stroud.

References

1. Abramson J, Smirnova I, Kasho V, Verner G, Kaback HR, and Iwata S. Structure and mechanism of the lactose permease of *Escherichia coli*. *Science* 301: 610–615, 2003.
2. Accardi A and Miller C. Secondary active transport mediated by a prokaryotic homologue of ClC Cl-channels. *Nature* 427: 803–807, 2004.
3. Andrade SL, Dickmanns A, Ficner R, and Einsle O. Crystal structure of the archaeal ammonium transporter Amt-1 from *Archaeoglobus fulgidus*. *Proc Natl Acad Sci USA* 102: 14994–14999, 2005.
4. Avent ND. A new chapter in Rh research: Rh proteins are ammonium transporters. *Trends Mol Med* 7: 94–96, 2001.
5. Avent ND. Molecular biology of the Rh blood group system. *J Pediatr Hematol Oncol* 23: 394–402, 2001.
6. Blakey D, Leech A, Thomas GH, Coutts G, Findlay K, and Merrick M. Purification of the *Escherichia coli* ammonium transporter AmtB reveals a trimeric stoichiometry. *Biochem J* 364: 527–535, 2002.
7. Broach J, Neumann C, and Kustu S. Mutant strains (nit) of *Salmonella typhimurium* with a pleiotropic defect in nitrogen metabolism. *J Bacteriol* 128: 86–98, 1976.
8. Conroy MJ, Bullough PA, Merrick M, and Avent ND. Modelling the human rhesus proteins: implications for structure and function. *Br J Haematol* 131: 543–551, 2005.
9. Conroy MJ, Jamieson SJ, Blakey D, Kaufmann T, Engel A, Fotiadis D, Merrick M, and Bullough PA. Electron and atomic force microscopy of the trimeric ammonium transporter AmtB. *EMBO J* 5: 1153–1158, 2004.
10. Durand A and Merrick M. In vitro analysis of the *Escherichia coli* AmtB-GlnK complex reveals a stoichiometric interaction and sensitivity to ATP and 2-oxoglutarate. *J Biol Chem* 281: 29558–29567, 2006.
11. Dutzler R, Campbell EB, Cadene M, Chait BT, MacKinnon R. X-ray structure of a ClC chloride channel at 3.0 A reveals the molecular basis of anion selectivity. *Nature* 415: 287–294, 2002.

12. Dutzler R, Campbell EB, and MacKinnon R. Gating the selectivity filter in ClC chloride channels. *Science* 300: 108–112, 2003.

13. Eyers SA, Ridgwell K, Mawby WJ, and Tanner MJ. Topology and organization of human Rh (rhesus) blood group-related polypeptides. *J Biol Chem* 269: 6417–6423, 1994.

14. Fu D, Libson A, Miercke LJ, Weitzman C, Nollert P, Krucinski J, and Stroud RM. Structure of a glycerol-conducting channel and the basis for its selectivity. *Science* 290: 481–486, 2000.

15. Gazzarrini S, Lejay L, Gojon A, Ninnemann O, Frommer WB, and von Wiren N. Three functional transporters for constitutive, diurnally regulated, and starvation-induced uptake of ammonium into *Arabidopsis* roots. *Plant Cell* 11: 937–948, 1999.

16. Granseth E, Daley DO, Rapp M, Melen K, and von Heijne G. Experimentally constrained topology models for 51,208 bacterial inner membrane proteins. *J Mol Biol* 352: 489–494, 2005.

17. Hackette SL, Skye GE, Burton C, and Segel IH. Characterization of an ammonium transport system in filamentous fungi with methylammonium-14C as the substrate. *J Biol Chem* 245: 4241–4250, 1970.

18. Harries WE, Akhavan D, Miercke LJ, Khademi S, and Stroud RM. The channel architecture of aquaporin 0 at a 2.2-A resolution. *Proc Natl Acad Sci USA* 101: 14045–14050, 2004.

19. Hemker MB, Cheroutre G, van Zwieten R, Maaskant-van Wijk PA, Roos D, Loos JA, van der Schoot CE, and von dem Borne AE. The Rh complex exports ammonium from human red blood cells. *Br J Haematol* 122: 333–340, 2003.

20. Holm LM, Jahn TP, Moller AL, Schjoerring JK, Ferri D, Klaerke DA, and Zeuthen T. NH_3 and NH_4^+ permeability in aquaporin-expressing *Xenopus* oocytes. *Pflügers Arch* 450: 415–428, 2005.

21. Howitt SM and Udvardi MK. Structure, function and regulation of ammonium transporters in plants. *Biochim Biophys Acta* 1465: 152–170, 2000.

22. Huang Y, Lemieux MJ, Song J, Auer M, and Wang DN. Structure and mechanism of the glycerol-3-phosphate transporter from *Escherichia coli*. *Science* 301: 616–620, 2003.

23. Jahn TP, Moller AL, Zeuthen T, Holm LM, Klaerke DA, Mohsin B, Kuhlbrandt W, and Schjoerring JK. Aquaporin homologues in plants and mammals transport ammonia. *FEBS Lett* 574: 31–36, 2004.

24. Javelle A and Merrick M. Complex formation between AmtB and GlnK: an ancestral role in prokaryotic nitrogen control. *Biochem Soc Trans* 33: 170–172, 2005.

25. Javelle A, Severi E, Thornton J, and Merrick M. Ammonium sensing in *Escherichia coli*. Role of the ammonium transporter AmtB and AmtB-GlnK complex formation. *J Biol Chem* 279: 8530–8538, 2004.

26. Javelle A, Thomas G, Marini AM, Kramer R, and Merrick M. In vivo functional characterization of the Escherichia coli ammonium channel AmtB: evidence for metabolic coupling of AmtB to glutamine synthetase. *Biochem J* 390: 215–222, 2005.

27. Jayakumar A and Barnes EM Jr. A filtration method for measuring cellular uptake of [^{14}C]methylamine and other highly permeant solutes. *Anal Biochem* 135: 475–478, 1983.

28. Jiang Y, Lee A, Chen J, Cadene M, Chait BT, and MacKinnon R. The open pore conformation of potassium channels. *Nature* 417: 523–526, 2002.

29. Khademi S, O'Connell J, 3rd Remis J, Robles-Colmenares Y, Miercke LJ, and Stroud RM. Mechanism of ammonia transport by Amt/MEP/Rh: structure of AmtB at 1.35 A. *Science* 305: 1587–1594, 2004.

30. Knepper MA. NH_4^+ transport in the kidney. *Kidney Int Suppl* 33: S95–S102, 1991.

31. Knepper MA, Packer R, and Good DW. Ammonium transport in the kidney. *Physiol Rev* 69: 179–249, 1989.

32. Kustu S and Inwood W. Biological gas channels for NH_3 and CO_2: evidence that Rh (Rhesus) proteins are CO_2 channels. *Transfus Clin Biol* 13: 103–110, 2006.

33. Lauter FR, Ninnemann O, Bucher M, Riesmeier JW, and Frommer WB. Preferential expression of an ammonium transporter and of two putative nitrate transporters in root hairs of tomato. *Proc Natl Acad Sci USA* 93: 8139–8144, 1996.

34. Lee JK, Khademi S, Harries W, Savage D, Miercke L, and Stroud RM. Water and glycerol permeation through the glycerol channel GlpF and the aquaporin family. *J Synchrotron Radiat* 11: 86–88, 2004.

35. Lee JK, Kozono D, Remis J, Kitagawa Y, Agre P, and Stroud RM. Structural basis for conductance by the archaeal aquaporin AqpM at 1.68 A. *Proc Natl Acad Sci USA* 102: 18932–18937, 2005.

36. Lin Y, Cao Z, and Mo Y. Molecular dynamics simulations on the *Escherichia coli* ammonia channel protein AmtB: mechanism of ammonia/ammonium transport. *J Am Chem Soc* 128: 10876–10884, 2006.

37. Liu K, Nagase H, Huang CG, Calamita G, and Agre P. Purification and functional characterization of Aquaporin-8. *Biol Cell* 98: 153–161, 2005.

38. Liu LH, Ludewig U, Gassert B, Frommer WB, and von Wiren N. Urea transport by nitrogen-regulated tonoplast intrinsic proteins in *Arabidopsis*. *Plant Physiol* 133: 1220–1228, 2003.

39. Liu Z, Chen Y, Mo R, Hui C, Cheng JF, Mohandas N, and Huang CH. Characterization of human RhCG and mouse Rhcg as novel nonerythroid Rh glycoprotein homologues predominantly expressed in kidney and testis. *J Biol Chem* 275: 25641–25651, 2000.

40. Liu Z and Huang CH. The mouse Rhl1 and Rhag genes: sequence, organization, expression, and chromosomal mapping. *Biochem Genet* 37: 119–138, 1999.

41. Liu Z, Peng J, Mo R, Hui C, and Huang CH. Rh type B glycoprotein is a new member of the Rh superfamily and a putative ammonia transporter in mammals. *J Biol Chem* 276: 1424–1433, 2001.

42. Marini AM, Boeckstaens M, Benjelloun F, Cherif-Zahar B, and Andre B. Structural involvement in substrate recognition of an essential aspartate residue conserved in Mep/Amt and Rh-type ammonium transporters. *Curr Genet* 49: 364–374, 2006.

43. Marini AM, Matassi G, Raynal V, Andre B, Cartron JP, and Cherif-Zahar B. The human Rhesus-associated RhAG protein and a kidney homologue promote ammonium transport in yeast. *Nat Genet* 26: 341–344, 2000.

44. Marini AM, Urrestarazu A, Beauwens R, and Andre B. The Rh (rhesus) blood group polypeptides are related to NH_4^+ transporters. *Trends Biochem Sci* 22: 460–461, 1997.

45. Meier-Wagner J, Nolden L, Jakoby M, Siewe R, Kramer R, and Burkovski A. Multiplicity of ammonium uptake systems in *Corynebacterium glutamicum*: role of Amt and AmtB. *Microbiology* 147: 135–143, 2001.

46. Merrick M, Javelle A, Durand A, Severi E, Thornton J, Avent ND, Conroy MJ, and Bullough PA. The *Escherichia coli* AmtB protein as a model system for understanding ammonium transport by Amt and Rh proteins. *Transfus Clin Biol* 13: 97–102, 2006.

47. Morais-Cabral JH, Zhou Y, and MacKinnon R. Energetic optimization of ion conduction rate by the K^+ selectivity filter. *Nature* 414: 37–42, 2001.

48. Musa-Aziz R, Chen LM, and Boron WF. Evidence from surface-pH transients that AmtB and RhAG, expressed in *Xenopus* oocytes, have a substantially lower CO_2/NH_3 permeability ratio than AQP1 (Abstract). *J Am Soc Nephrol*, 2006.

49. Nakhoul NL and Hamm LL. Non-erythroid Rh glycoproteins: a putative new family of mammalian ammonium transporters. *Pflügers Arch* 447: 807–812, 2004.

50. Nielsen H, Engelbrecht J, Brunak S, and von Heijne G. A neural network method for identification of prokaryotic and eukaryotic signal peptides and prediction of their cleavage sites. *Int J Neural Syst* 8: 581–599, 1997.

51. Ninnemann O, Jauniaux JC, and Frommer WB. Identification of a high affinity NH_4^+ transporter from plants. *EMBO J* 13: 3464–3471, 1994.

52. Pao SS, Paulsen IT, and Saier MH Jr. Major facilitator superfamily. *Microbiol Mol Biol Rev* 62: 1–34, 1998.

53. Park JH and Saier MH Jr. Phylogenetic characterization of the MIP family of transmembrane channel proteins. *J Membr Biol* 153: 171–180, 1996.

54. Priver NA, Rabon EC, and Zeidel ML. Apical membrane of the gastric parietal cell: water, proton, and nonelectrolyte permeabilities. *Biochemistry* 32: 2459–2468, 1993.

55. Quentin F, Eladari D, Cheval L, Lopez C, Goossens D, Colin Y, Cartron JP, Paillard M, and Chambrey R. RhBG and RhCG, the putative ammonia transporters, are expressed in the same cells in the distal nephron. *J Am Soc Nephrol* 14: 545–554, 2003.

56. Rapp M, Granseth E, Seppala S, and von Heijne G. Identification and evolution of dual-topology membrane proteins. *Nat Struct Mol Biol* 13: 112–116, 2006.

57. Ridgwell K, Eyers SA, Mawby WJ, Anstee DJ, and Tanner MJ. Studies on the glycoprotein associated with Rh (rhesus) blood group antigen expression in the human red blood cell membrane. *J Biol Chem* 269: 6410–6416, 1994.

58. Ripoche P, Bertrand O, Gane P, Birkenmeier C, Colin Y, and Cartron JP. Human Rhesus-associated glycoprotein mediates facilitated transport of NH(3) into red blood cells. *Proc Natl Acad Sci USA* 101: 17222–17227, 2004.

59. Roos A and Boron WF. Intracellular pH. *Physiol Rev* 61: 296–434, 1981.

60. Saier MH Jr, Eng BH, Fard S, Garg J, Haggerty DA, Hutchinson WJ, Jack DL, Lai EC, Liu HJ, Nusinew DP, Omar AM, Pao SS, Paulsen IT, Quan JA, Sliwinski M, Tseng T-T, Wachi S, and Young GB. Phylogenetic characterization of novel transport protein families revealed by genome analyses. *Biochim Biophys Acta* 1422: 1–56, 1999.

61. Savage DF, Egea PF, Robles-Colmenares Y, O'Connell JD 3rd, and Stroud RM. Architecture and selectivity in aquaporins: 2.5 a X-ray structure of aquaporin Z. *PLoS Biol* 1: E72, 2003.

62. Soupene E, Chu T, Corbin RW, Hunt DF, and Kustu S. Gas channels for NH(3): proteins from hyperthermophiles complement an *Escherichia coli* mutant. *J Bacteriol* 184: 3396–3400, 2002.

63. Soupene E, He L, Yan D, and Kustu S. Ammonia acquisition in enteric bacteria: physiological role of the ammonium/methylammonium transport B (AmtB) protein. *Proc Natl Acad Sci USA* 95: 7030–7034, 1998.

64. Soupene E, Inwood W, and Kustu S. Lack of the Rhesus protein Rh1 impairs growth of the green alga *Chlamydomonas reinhardtii* at high CO_2. *Proc Natl Acad Sci USA* 101: 7787–7792, 2004.

65. Soupene E, Lee H, and Kustu S. Ammonium/methylammonium transport (Amt) proteins facilitate diffusion of NH_3 bidirectionally. *Proc Natl Acad Sci USA* 99: 3926–3931, 2002.

66. Sui H, Han BG, Lee JK, Walian P, and Jap BK. Structural basis of water-specific transport through the AQP1 water channel. *Nature* 414: 872–878, 2001.

67. Thomas G, Coutts G, and Merrick M. The glnKamtB operon. A conserved gene pair in prokaryotes. *Trends Genet* 16: 11–14, 2000.

68. Thomas GH, Mullins JG, and Merrick M. Membrane topology of the Mep/Amt family of ammonium transporters. *Mol Microbiol* 37: 331–344, 2000.

69. Van den Berg B, Clemons WM Jr, Collinson I, Modis Y, Hartmann E, Harrison SC, and Rapoport TA. X-ray structure of a protein-conducting channel. *Nature* 427: 36–44, 2004.

70. Van Kim CL, Colin Y, and Cartron JP. Rh proteins: key structural and functional components of the red cell membrane. *Blood Rev* 20: 93–110, 2005.

71. von Wiren N, Bergfeld A, Ninneman O, and Frommer WB. Sequence announcement. *Plant Mol Biol* 35: 681, 1997.

72. von Wiren N, Gazzarrini S, Gojon A, and Frommer WB. The molecular physiology of ammonium uptake and retrieval. *Curr Opin Plant Biol* 3: 254–261, 2000.

73. Weiner ID and Verlander JW. Renal and hepatic expression of the ammonium transporter proteins, Rh B Glycoprotein and Rh C Glycoprotein. *Acta Physiol Scand* 179: 331–338, 2003.

74. Westhoff CM, Ferreri-Jacobia M, Mak DO, and Foskett JK. Identification of the erythrocyte Rh blood group glycoprotein as a mammalian ammonium transporter. *J Biol Chem* 277: 12499–12502, 2002.

75. Yamashita A, Singh SK, Kawate T, Jin Y, and Gouaux E. Crystal structure of a bacterial homologue of Na^+/Cl^--dependent neurotransmitter transporters. *Nature* 437: 215–223, 2005.

76. Zheng L, Kostrewa D, Berneche S, Winkler FK, and Li XD. The mechanism of ammonia transport based on the crystal structure of AmtB of *Escherichia coli*. *Proc Natl Acad Sci USA* 101: 17090–17095, 2004.